PORE-SCALE NETWORK MODELING OF SHARP AND DIFFUSE INFILTRATION FRONTS THROUGH THE ADDITION OF VISCOUS EFFECTS

DAVID A. DICARLO[1]

[1] *National Sedimentation Laboratory, Agricultural Research Service, U.S. Department of Agriculture, PO Box 1157, Oxford, Mississippi*

ABSTRACT

Most infiltrations of a wetting phase have an imbibition front that is diffuse at the pore-scale, allowing the common use of continuum formulations to model the macroscopic flow. But for macroscopic flow phenomena such as preferential flow, this continuum approach fails as the imbibition water front is sharp at the pore-scale. Pore-scale network models are ideal for handling sharp fronts due to their inherent discreteness, but many models produce only sharp fronts contrary to observations. Here we modify the physically-based static network model of Valvatne and Blunt to add viscous effects in a quasi-static manner. We find that at low imbibition velocities, that the imbibing front is diffuse due to flow within the layers of the model, and the majority of the elements filling through snap-off. At high imbibition velocities, the front becomes sharp at the pore-scale due to the viscous forces enhancing collective piston-like pore filling. The width of the transition between diffuse and sharp fronts in terms of velocity matches well what is observed in experimental measurements. We discuss how the initial layer conductivity, pore-size distribution, and the wetting properties of the media control the absolute magnitude of the transition.

1. INTRODUCTION

Water infiltrating into uniform water-wet porous media has been observed to produce a phenomena where the saturation and pressure profiles show a non-monotonic (or overshoot) behaviour for certain initial and boundary conditions (Stonestrom and Akstin 1994, Geiger and Durnford 2000, DiCarlo 2004, Shiozawa and Fujimaki 2004). It has been argued that saturation overshoot is a necessary condition to produce flow phenomena such as gravity driven fingering (Raats 1973, Eliassi and Glass 2001). Saturation overshoot has been found to occur only for imbibing fluxes above a certain critical flux where this critical flux depends on parameters such as the initial saturation of the media, and the size, shape and distribution of the grains of the media (DiCarlo 2004).

It has been suggested that overshoot occurs when the infiltrating front is abrupt at the pore-scale leading to a sharp jump in saturation and possibly oversaturation. If the front is diffuse, then the medium can wet to the correct saturation to carry the flux without oversaturating. In this explanation, the minimum saturation behind a sharp wetting front is controlled by the pore-scale filling processes. Using micro-models of porous media, Lenormand and Zarcone (1984) observed that at high frontal velocities the wetting front is very sharp with almost all pores filled directly behind the front. At very low frontal velocities, the front is diffuse with many pores and throats remaining unfilled behind the front.

Lenormand and Zarcone (1984) explained this phenomenon in terms of a competition between piston-like collective filling at the main front and filling ahead of the front due to conduction through water layers in the corners of the pore space (see also Blunt and Scher (1995)). This picture has been observed in pore-scale observations on infiltration into glass bead porous media (Lu et al. 1994).

To scale up observed pore-scale filling processes (such as those discussed above) to macroscopic flow properties which included thousands of pores, network models are often used (Blunt 2001). The exact details of the network model are important for simulating the observed overshoot behavior. Network models where elements can only be filled or unfilled show abrupt fronts at all velocities (Glass et al. 1998). In contrast, traditional network models where elements can be partially filled always produce diffuse fronts. This paper uses a state of the art network model (Valvatne and Blunt 2004, Valvatne et al. 2005) with geologically determined pore and throat connections, and non-circular elements that allow corner flow. To this static model, dynamic viscous forces are added using an approach pioneered by Hughes and Blunt (2000) and Blunt and Scher (1995). It is found that by including viscous forces, there is a transition flux above which the infiltration front is sharp at the pore-scale, and below which the infiltration front is diffuse. The flux at which the transition between diffuse and sharp fronts takes place has previously been found to compare well to experimental measurements of overshoot (DiCarlo 2006). In this paper, the model is summarized, and we report on how wettability, porous media grain size and distribution, and initial water content affect the transition flux, and its dependence on initial conductivity of the medium.

2. VISCOUS NETWORK MODEL

For capillary dominated displacements (with viscous and gravitational forces being negligible at the pore-scale), network models often use a rule based method for moving fluid through the network (Blunt 2001). These models are quasi-static in the sense that when capillary forces make an element energetically favorable to be filled with fluid, it is filled with no consideration of the forces that are needed to move the fluid into position. This is a reasonable assumption if the flow rate is very slow, but even at moderate flow rates, the viscous forces that move the fluids to the element need to be added. In contrast, dynamic network modeling uses algorithms where the pressure field is updated within a pore filling (Mogensen et al. 1999, Al-Gharbi and Blunt 2005). These algorithms tend to be much more computationally expensive and severely limit the size of the network that can be used. The network model described below is quasi-static, but incorporates dynamic viscous effects in a straightforward manner to allow computations on a large network for comparisons to experiments. This method was pioneered by Blunt and Scher (1995) and recently updated by Hughes and Blunt (2000). Recently, another quasi-static method has been used by Nguyen et al. (Nguyen et al. 2004, 2005), where they assume that there are no pressure gradients within the bulk fluid, but the gradients in the fluid in the corners are non-negligible.

The viscous network model used in this study is based on the state of the art network model of Valvatne et al. (Valvatne and Blunt 2004, Valvatne et al. 2005). This model includes a realistic connection topology of the pores and throats, non-circular elements that allow the wetting fluid (hereafter called water) to be retained in the corners of the element even when the main body of the element is filled with non-wetting fluid (hereafter called gas), and both snap-off and collective pore filling as imbibition processes.

In network models, the capillary pressure (P_c) controls the element filling process and thus the displacement. For static models, P_c is the same throughout the network as it is assumed that capillary forces dominate on the pore-scale. In this viscous model, the capillary pressure varies along the model during imbibiton as at high flow rates P_c will be low near the water inlet (high water pressure) and high near the outlet. This local water pressure is calculated as follows. Before any elements are filled, the conductivity of each element to a particular phase (water or gas) is calculated from the amount of phase that exists in the element, and the size and shape of the element. The input flux is applied across the network, and the water pressure (and capillary pressure) in each element is calculated. This is then the new starting basis for the next round of pore filling using the static network model rules (albeit with the correct pressures). Approximately 100 element fills occur before recalculating the pressure field across the network as this is the most expensive computational step, and for a model of this size (38,495 elements) this does not noticeably affecting the filling pattern.

The pore-space geometry was chosen to be from a network based on a Berea sandstone (Øren and Bakke 2003). This consisted of a three-dimensional network with 12,349 pores and 26,146 throats. The pore and throat size distribution of the sandstone was scaled to match the experimental sands. A truncated Weibull distribution

$$r_t = (r_{t,\max} - r_{t,\min})(-\delta \ln[\beta(1-e^{-1/\delta}) + e^{-1/\delta}])^{1/\gamma} + r_{t,\min} \quad (1)$$

was used for the throat radius (r_t) distribution, where β is a random number between 0 and 1, δ = 0.13, γ = 1.4. The pore radii were determined from the average connecting throat radii scaled by the aspect ratio α obtained fromanother truncated Weibull distribution (δ = 0.09, γ = 2.0, α_{max} = 4.81, and α_{min} = 1.03). For 20/30 sand (the basis sand), values of $r_{t,min}$=0.050 mm, $r_{t,max}$=0.400 mm give a very good fit to the static imbibition and drainage P-S curves.

To compare with experimental infiltrations, model infiltrations were run on the network models with pore sizes corresponding to initially dry 12/20, 20/30, and 30/40 sands. Likewise, variations in pore-size distribution, initial water content, and wettability are listed in Table 1. For all initially dry media, the model was set to have an initial capillary pressure of 9 kPa to achieve an initial water connection.

TABLE 1. Relevant starting parameters for the various simulation runs, and the resulting transition fluxes. The retention parameters shown are for imbibition.

Sand	variation	$r_{t,min}$ mm	$r_{t,max}$ mm	θ	K cm/min	K_i x10^{-3} cm/min	α cm^{-1}	n	q_{min} x10^{-3} cm/min	q_{max} x10^{-3} cm/min
20/30	basis	0.05	0.40	0°	14	0.0093	0.20	4.2	12	43
12/20	size	0.07	0.56	0°	28	0.0048	0.29	5.3	5	23
30/40	size	0.04	0.31	0°	8.6	0.0154	0.16	3.7	23	83
20/30	distribution	0.02	0.52	0°	14	0.0102	0.24	2.9	13	47
20/30	distribution	0.01	0.80	0°	14	0.0124	0.29	2.5	17	70
20/30	initial water	0.05	0.40	0°	14	2.5200	0.20	4.2	600	2200
20/30	wettability	0.05	0.40	35°	14	0.0093	0.26	4.0	10	35
20/30	wettability	0.05	0.40	70°	14	0.0093	0.07	4.8	3.5	12

3. RESULTS

Figure 1a shows four snapshot slices of the infiltration pattern in the network model for four fluxes, q = 0.010, 0.017, 0.023, and 0.038 cm/min into dry, water-wet, 20/30 sand. Water entered the left side of the model and gas exited the right side. In each case the snapshot of the pattern was taken when the wetting front was approximately 40% into the model. The water filled pore elements are depicted with solid circles, and the connecting throat elements with solid lines. Gas filled elements are not shown. For the lowest flux shown (q = 0.010 cm/min), the wetting front is relatively diffuse and the water filled elements are primarily throats which are filled through the snap-off mechanism. For the highest flux shown (q = 0.038 cm/min), behind the wetting front almost all of the elements are water filled (both pores and throats), with over 90% filled through the piston-like mechanism. For the intermediate fluxes of q = 0.017 and q = 0.023 cm/min, there still exists a somewhat sharp front, but behind the front only a portion of the elements are filled.

To observe how the fronts move through the model, the saturation within 20 slices normal to the flow direction is calculated after a certain number of filling events. This allows depictions of saturation versus distance and time, rather than just a single snapshot. Using the same fluxes as in Fig. 1a, Figure 1b shows the simulation results in terms of saturation versus distance in the model. For the highest flux shown (and all higher fluxes), at a particular point the saturation jumps from its initial value to its final value (near saturation) as the front moves through. No intermediate saturations are reached. For intermediate fluxes, the sharp front and the saturation jump occur, just not to complete saturation. For the lowest flux shown (and all lower fluxes), the saturation moves continuously up from the initial saturation with a diffuse rather than abrupt front.

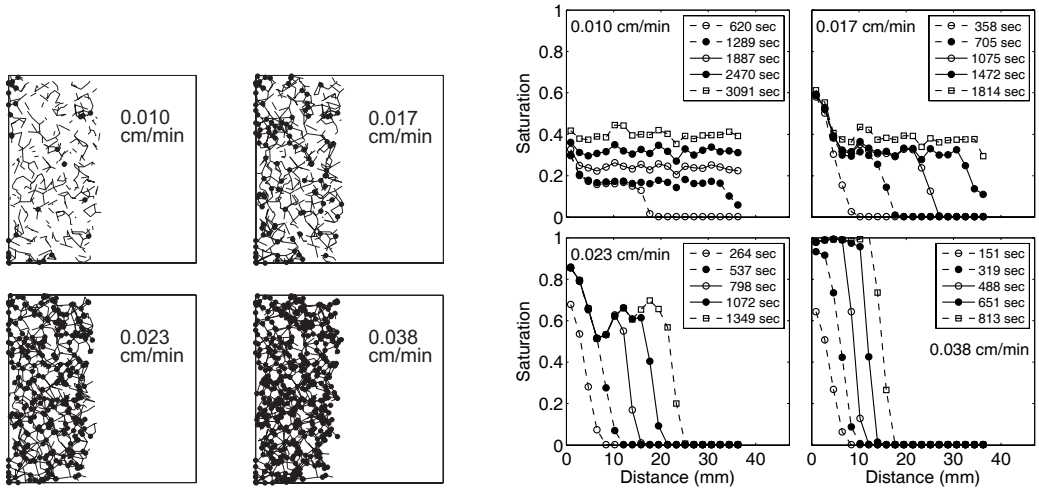

FIGURE 1. a) Two-dimensional representations of the pores (solid circles) and throats (line segments) that are water filled when the initial front is 40% of the way across the network model for four different fluxes. Low fluxes show a diffuse front with mainly pores filled, while high fluxes a completely filled front. b) The saturation profiles obtained at different times for the four fluxes.

Importantly, the saturation behind the front in the network model is the minimum saturation that can be attained macroscopically, and this saturation is a function of the flux. At low fluxes, all saturations are attainable, at intermediate fluxes, only saturations above the saturation at the front are attainable, and at high fluxes, the saturation jumps to complete saturation due to the viscous effects in the model. Figure 2a shows a plot of the predicted minimum saturation behind the front versus flux for dry 20/30 sand (solid line). This minimum saturation is obtained by averaging the saturation observed in each slice normal to the flow direction behind the front. For fluxes below 0.01 cm/min, there was no observable front, and thus there is no minimum saturation behind the front. The data from the model is compared to the tip saturation (i.e. the saturation directly behind the front) measured experimentally. As can be seen, an initial capillary pressure of 9 kPa for the dry sand (initial water saturation of S_i = 1.5x10^{-3}) provides a reasonable fit to the transition flux between overshoot and no overshoot. The overshoot saturation is not matched nearly as well, as the network model predicts almost complete filling behind the front while the experimental data suggest that the filling behind the front is somewhat incomplete at moderate to high fluxes.

Along with the initially dry sands, overshoot was measured in the 20/30 sand when it was prewet to a saturation of S_i = 0.028 (equal to the 0.01 volumetric water content in the experimental study). Figure 2b shows the model results in comparison to the experimental results for 20/30 sand with S_i = 0.028. Importantly, for the network model in this case, there are no adjustable parameters, as the initial saturation is fixed. With this initial saturation, overshoot is not seen in the network model until fluxes greater than 1 cm/min. This transition flux is close to that seen in the experimental measurements. Again, above this flux, the network model predicts complete saturation behind the front, while the experimental measurements show less than complete saturation. For a higher initial saturation (S_i = 0.056), the network model does not show an abrupt front below the saturated conductivity (15 cm/min) which also matches the experimental data (not shown in a figure).

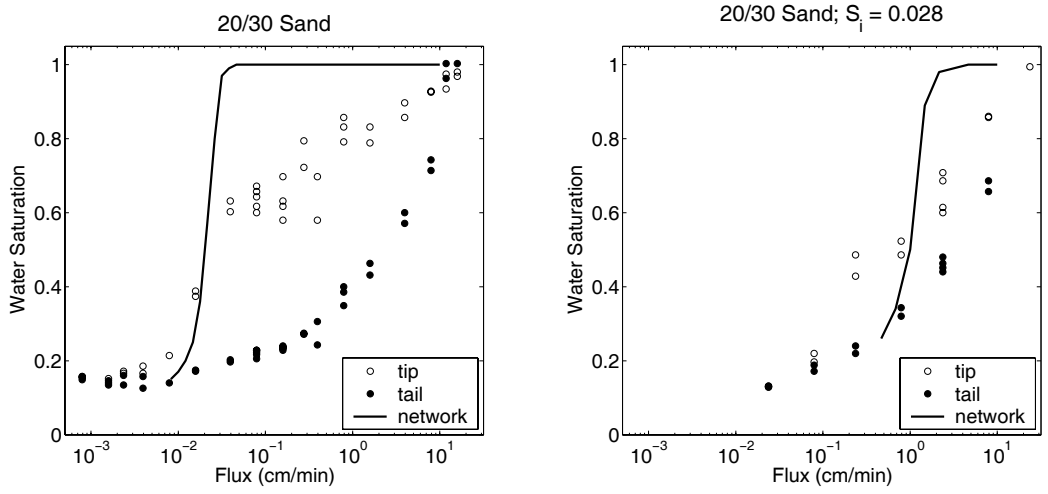

FIGURE 2. a) Network model prediction of the saturation directly behind the front (solid line) as a function of applied flux for dry 20/30 sand. This is compared to the experimental measurements of the saturation directly behind the front (open circles) during infiltration. b) The same plot except for sand with an initial saturation of 0.028. Initial saturation moves the transition flux to 1cm/min, with a broader transition to fully filled.

The network model can be scaled to reproduce the pore and throat sizes of a coarser grained 12/20 sand and a finer grained 30/40 sand. The overall connections and shapes of the elements are kept the same as used for the morphologically similar 20/30 sand. The same capillary pressure (9 kPa) is used as an initial condition. This is found to reproduce the experimental data well for the two other sands, with a lower transition flux (0.005 cm/min) for the coarser 12/20 sand, and a higher transition flux (0.023 cm/min) for the finer 30/40 sand. Due to the smaller elements being filled at the same capillary pressure, the initial conductivity of the 12/20 sand is also lower than the initial conductivity of the 30/40 sand. This point will be discussed later as the initial conductivity plays a large role in interpreting the results.

In addition to size of the media affecting the transition flux, the pore-size distribution and wettability of the media may also affect the transition flux. The model was run using parameters that resulted in a medium with the same permeability as the 20/30 sand, but with a broader pore distribution than the 20/30 sand. This is reflected in the smaller *n* values in the retention curve fits. Figure 3a shows how the transition is affected for the three pore size distributions as the broader pore size distributions resulted in slightly higher transition fluxes, and a slightly broader transition. Also, the wettability of the model media was adjusted by increasing the air-water-solid contact angle from 0° to 35° and 70°. Figure 3b shows how the contact angle affects the transition between the diffuse and sharp wetting front. A contact angle of 35° lowers the transition flux by a factor of 1.25, while a contact angle of 70° lowers the transition flux by a factor of 4. Higher contact angles were not able to be simulated.

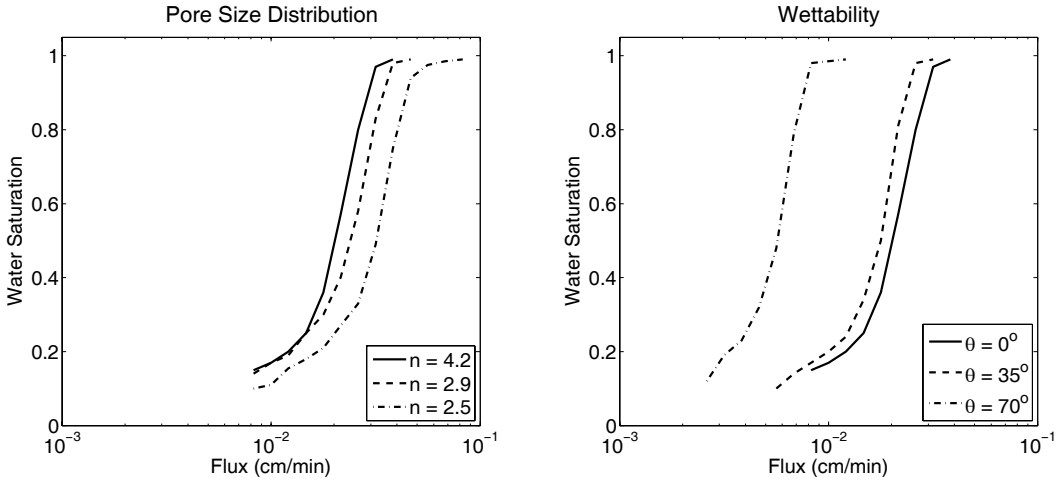

FIGURE 3. a) A broader pore size distribution (lower *n* in the van Genuchten fits) shifts the transition to higher fluxes. b) A higher contact angle (less water-wet) shifts the transition to lower fluxes, with much of the shift happening above a contact angle of 60°.

4. DISCUSSION

All of the simulations show there is a transition between diffuse and sharp wetting fronts, and this transition depends on initial saturation, grain size, grain size distribution, and wetting properties of the porous medium. Table 1 lists the relevant parameters and results for all of the model runs shown. In all the runs, there are two transition fluxes; one, a minimum flux (q_{min})

below which no differences are observed between the static model and the dynamic model (i.e. viscous effects are negligible, and the front is diffuse across the entire model), and two, a maximum flux (q_{max}) above which the pore filling behind the front is complete, and the water phase moves like a piston-like displacement through the model. As shown in the table these transition fluxes are highly correlated with the initial conductivity of the media, with the exception of the wettability changes. This is intuitive as this initial conductivity effectively sets the flow scale for the viscous effects. In fact, for most of the changes the model results suggest that q_{min} is linearly dependent on the initial conductivity

$$q_{\min} = CK_i \ , \tag{2}$$

where the proportionality constant C depends slightly on the porous medium. For initially dry media, it varies from 1000 for the coarse 12/20 sand to 1500 for the finer 30/40 sand. It is much lower for partially wet media (approximately 200), and slightly greater for the medium with a broader pore distribution.

In previous studies of the transition between diffuse and sharp wetting fronts (Hughes and Blunt, 2000), viscous effects are assumed to be correlated with the capillary number

$$Ca = \frac{\mu q}{\sigma} \ , \tag{3}$$

(where μ is the viscosity and σ is the surface tension) rather than the initial conductivity. Traditionally, it is believed the capillary number needs to be about 10^{-4} before viscous forces become capillary forces at the pore scale (Dullien 1992). This study and the experimental results, show that the creation of sharp fronts and overshoot through viscous effects is seen at capillary numbers down to 10^{-8}, a capillary number of about 4 orders of magnitude smaller than when the forces become comparable at the pore scale. Thus besides the capillary number this study suggests that an additional criterion for when viscous forces become significant is when the infiltrating flux is 3 orders of magnitude greater than the initial conductivity, at least for imbibition. In regards to wettability, the higher contact angles (less water-wet media) will preferentially suppress snap-off as this filling process is much more dependent on contact angle than the piston-like filling process. This is minor below contact angles of 60°, but increases quickly above it. Thus, we observe lower transition fluxes with increasing contact angles, as the front becomes sharper with more piston-like filling. Presumably, for contact angles above 90° snap-off will be fully repressed, and the front may be sharp for all fluxes.

The scaling between the transition flux and the initial conductivity explains why overshoot and sharp fronts at the pore scale are not seen in most infiltrations into porous media. Viscous effects and overshoot only occur if the imbibing flux is 3 orders of magnitude greater than the initial conductivity or if the media is water repellent. If the media is pre-wet or has a broad pore size distribution, the initial conductivity will be non-negligible, and the transition to sharp fronts will only occur at fluxes greater than the saturated conductivity of the media.

In conclusion, it is shown that a physically-based network model with viscous pressure drops predicts that for infiltration that there exists a transition flux between diffuse and sharp fronts, and that this prediction matches well with experimental data. Increasing repellency of the media drastically reduces the transition flux above contact angles of 60°, while broader

pore-size distributions increase the transition flux. These results are consistent with qualitative observations of infiltrating fronts.

REFERENCES

- Al-Gharbi, M. S., and M. J. Blunt. 2005. Dynamic network modeling of two-phase drainage in porous media. Physical Review E - Statistical, Nonlinear, and Soft Matter Physics 71:1-16.
- Blunt, M. J. 2001. Flow in porous media - Pore-network models and multiphase flow. Current Opinion in Colloid and Interface Science 6:197-207.
- Blunt, M. J., and H. Scher. 1995. Pore-level modeling of wetting. Physical Review E 52:6387-6403.
- de Gennes, P. G. 1985. Wetting: statics and dynamics. Review of Modern Physics 57:827-863.
- DiCarlo, D. A. 2004. Experimental measurements of saturation overshoot on infiltration. Water Resources Research 40:W04215, doi:04210.01029/02003WR002670.
- DiCarlo, D. A. 2006. Quantitative Network Model Predictions of Saturation Behind Infiltration Fronts and Comparison to Experiments. Water Resources Research (in press).
- Dullien, F. A. L. 1992. Porous Media: Fluid Transport and Pore Structure, 2nd edition. Academic Press, Inc., San Diego, CA.
- Eliassi, M., and R. J. Glass. 2001. On the continuum-scale modeling of gravity-driven fingers in unsaturated porous media: The inadequacy of the Richards equation with standard monotonic constitutive relations and hysteretic equations of state. Water Resources Research 37:2019-2035.
- Geiger, S. L., and D. S. Durnford. 2000. Infiltration in homogeneous sands and a mechanistic model of unstable flow. Soil Science Society of America Journal 64:460-469.
- Glass, R. J., M. J. Nicholl, and L. Yarrington. 1998. A modified invasion percolation model for low-capillary number immiscible displacements in horizontal rough-walled fractures: Influence of local in-plane curvature. Water Resources Research 34:3215-3234.
- Hughes, R. G., and M. J. Blunt. 2000. Pore scale modeling of rate effects in imbibition. Transport in Porous Media 40:295-322.
- Lenormand, R., and C. Zarcone. 1984. Role of roughness and edges during imbibition in square capillaries. paper SPE 13264 presented at the 59th Annual Technical Conference of the SPE, Houston, TX, September 16-19.
- Lu, T. X., J. W. Biggar, and D. R. Nielsen. 1994. Water movement in glass bead porous media 2. Experiments of infiltration and finger flow. Water Resources Research 30:3283-3290.
- Mason, G., and N. R. Morrow. 1991. Capillary behavior of a perfect wetting liquid in irregular triangular tubes. Journal of Colloid and Interface Science 141:262-274.
- Mogensen, K., E. Stenby, S. Banerjee, and V. A. Barker. 1999. Comparison of iterative methods for computing the pressure field in a dynamic network model. Transport in Porous Media 37:277-301.
- Nguyen, V. H., A. P. Sheppard, M. A. Knackstedt, and W. Val Pinczewski. 2004. A dynamic network model for imbibition. SPE International Petroleum Conference in Mexico - Proceedings:215-235.
- Nguyen, V. H., A. P. Sheppard, M. A. Knackstedt, and W. Val Pinczewski. 2005. The effects of displacement rate and wettability on imbibition relative permeabilities. SPE Annual Technical Conference and Exhibition in Dallas, TX - Proceedings Paper SPE 95953.
- Øren, P.-E., and S. Bakke. 2003. Reconstruction of Berea sandstone and pore-scale modelling of wettability effects. Journal of Petroleum Science and Engineering 39:177-199.
- Raats, P. A. C. 1973. Unstable wetting fronts in uniform and nonuniform soils. Soil Science Society of America Proceedings 37:681-686.
- Stonestrom, D. A., and K. C. Akstin. 1994. Nonmonotonic matric pressure histories during constant flux infiltration into homogeneous profiles. Water Resources Research 30:81-91.
- Valvatne, P. H., and M. J. Blunt. 2004. Predictive pore-scale modeling of two-phase flow in mixed wet media. Water Resources Research 40:W07406, doi:07410.01029/02003WR002627.
- Valvatne, P. H., M. Piri, X. Lopez, and M. J. Blunt. 2005. Predictive pore-scale modeling of single and multiphase flow. Transport in Porous Media 58:23-41.